PERGAMON

International Journal of Solids and Structures 38 (2001) 435–443

INTERNATIONAL JOURNAL OF SOLIDS and STRUCTURES

www.elsevier.com/locate/ijsolstr

Shear–bending–torsion elastic interaction diagrams in circular steel sections

R. Irles Más *, F. Irles Más

Department of Civil Engineering, University of Alicante, Apdo. Correos 99, E-03080 Alicante, Spain

Received 16 December 1999

Abstract

Interaction diagrams are extensively used as a tool for designing prismatic members subjected to several combined stresses. For a long time, sets of these diagrams have been available in building technologies, such as reinforced concrete, steel and composite sections, under various stresses.

This paper shows the analytical formulation to obtain the diagrams corresponding to bending and torsion simultaneously acting on steel circular cross-sections in combination with shear force. In particular, a detailed analysis of the interaction elastic limit surface is carried out for stresses acting on circular sections. © 2000 Elsevier Science Ltd. All rights reserved.

Keywords: Interaction limit surface; Shear–bending–torque; Circular steel section

1. Introduction

This paper develops a topic within the same field as the one recently presented by the same authors (Irles and Irles, 2000), but includes the study and construction of interaction diagrams for circular sections with shear–bending–torsion.

This present study has the peculiarity that the interaction surface is made up of two regions with different characteristics (one of them is flat) depending on the different locations of the most stressed point in the section. These positions correspond to different relative preponderance intervals of certain stresses among those considered.

2. Approach to the problem

2.1. Yielding condition

Fig. 1 shows the stresses in a circular section generated by a torque (T), bending moment (F), and shear force (Q).

* Corresponding author. Fax: +34-9-6590-3678.
E-mail address: dicop@ua.es (R. Irles Más).

PII: S0020-7683(00)00046-9

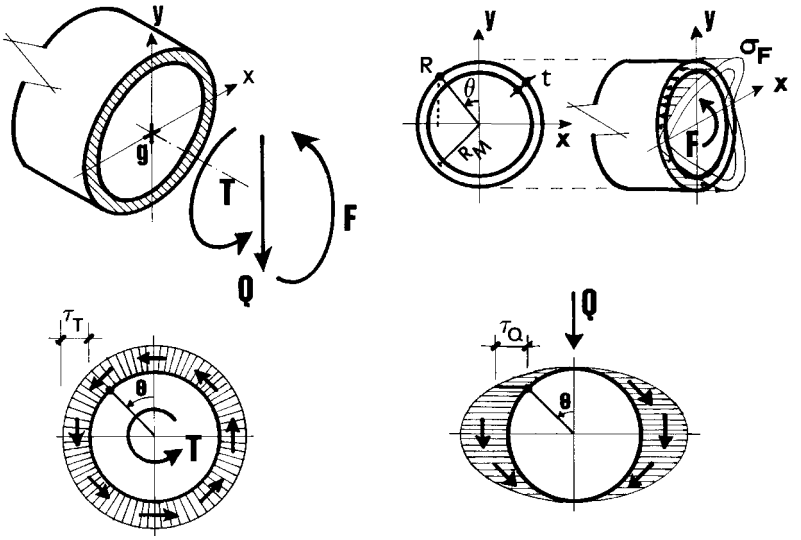

Fig. 1. Stresses in the circular section.

The analytical expression of the corresponding stresses is

$$\sigma_F = \frac{F}{I_F} R\cos\theta = \frac{2F}{I_T} R\cos\theta = \frac{2F}{W}\cos\theta, \tag{1a}$$

$$\tau_T = \frac{T}{I_T} R = \frac{T}{W}, \tag{1b}$$

$$\tau_Q = \frac{QM_{EST}}{tI_F} = 2\frac{QR_M^2\sin\theta}{RW}, \tag{1c}$$

where the terms in the expressions are defined as follows: $W = I_T/R$ is the torsional resistant modulus, I_F, the moment of inertia and $I_T = 2I_F$, the torsional modulus, t, the thickness, R, the outer radius and R_M, the midline one, $M_{EST} = \int_0^\theta tR_M^2\cos\theta\,d\theta$, the first-order static moment about bending axis, and τ_Q, the average for the shear stress τ at each point in the wall's mid-line (this expression becomes less precise when the thickness increases).

The effective stress at a generic point on the outer contour line (where it will no doubt find its maximum value) is expressed below:

$$\sigma_{co} = \sqrt{\sigma^2 + 3\tau^2} = \sqrt{\left(\frac{2F\cos\theta}{W}\right)^2 + 3\left(\frac{T + 2QR_0\sin\theta}{W}\right)^2} = \sqrt{f(\theta)},$$

where $R_0 = R_M^2/R$, and with respect to the only variable θ, which defines the position of the point considered.

Following the usual yield criterion according to which the effective stress at the point (θ_{max}) with the highest stress will reach the elastic limit σ_e, this condition will be

$$\sigma_e = \sqrt{f(\theta_{max})}$$

or

$$\sigma_e^2 = f(\theta_{max}) = (4F^2\cos^2\theta_{max} + 3T^2 + 12TQR_0\sin\theta_{max} + 12Q^2R_0^2\sin^2\theta_{max})/W^2. \quad (2)$$

2.2. The search for the most stressed point

Since the stress functions (1) are continuous and valid throughout the range $\theta \in [0, 2\pi]$, the value of θ_{max} can be obtained using the mathematical maximum condition:

$$f'(\theta) = 0 = (-8F^2\sin\theta\cos\theta + 12TQR_0\cos\theta + 24Q^2R_0^2\sin\theta\cos\theta)/W^2. \quad (3)$$

This equation has two solutions in the interval $\theta \in [0, \pi/2]$ (keeping in mind that it will suffice to look for the maximum value at that interval and taking into account the sign convention considered for Q and T, and the symmetry of the problem):

$$\text{(a)} \quad \cos\theta = 0 \;\Rightarrow\; \theta_1 = \frac{\pi}{2}. \quad (4)$$

This first solution for θ_{max} always occurs, regardless of the values of T, F and Q. However, it will be shown that it cannot always be a maximum. The second solution is

$$\text{(b)} \quad -8F^2\sin\theta + 12TQR_0 + 24Q^2R_0^2\sin\theta = 0 \;\Rightarrow\; \theta_2 = \arcsin\frac{3TQR_0}{2F^2 - 6Q^2R_0^2}. \quad (5)$$

This solution is only real when $\left[3TQR_0/\left(2F^2 - 6Q^2R_0^2\right)\right] \in [0, 1]$, or (restricting it to positive values of T, F and Q given the symmetry of the problem) when simultaneously

$$2F^2 - 6Q^2R_0^2 > 0, \quad (6a)$$

$$3TQR_0 \leqslant 2F^2 - 6Q^2R_0^2 \rightarrow\; C_1(T, F, Q) = 6Q^2R_0^2 + 3TQR_0 - 2F^2 \leqslant 0. \quad (6b)$$

This solution adopts two particular values: $\theta_2 = \theta_1 = \pi/2$ when Eq. (6b) is strictly fulfilled ($C_1 = 0$) and $\theta_2 = 0$ when either T or Q is zero.

2.3. Discussion of maximum values

The local maxima correspond to (T, F, Q) values making the second derivative strictly negative:

$$f''(\theta) = \left[\left(24Q^2R_0^2 - 8F^2\right)\cos 2\theta - 12TQR_0\sin\theta\right]/W^2 < 0. \quad (7)$$

For each case, the following applies:

$$\text{(a)} \quad f''(\pi/2) = \left(8F^2 - 24Q^2R_0^2 - 12TQR_0\right)/W^2 < 0.$$

This will occur, simplifying common factors, when

$$C_1 = 6Q^2R_0^2 + 3TQR_0 - 2F^2 > 0. \quad (8)$$

Only in that region of (T, F, Q) space is there a local maximum in $\theta_1 = \pi/2$ (outside, there is a minimum at the same point, since the first derivative is always zero at this point; at the border of region, $C_1 = 0$, the function $f(\theta)$ lacks a curvature; however, being symmetrical with respect to θ_1, it does not show an inflexion point but it will be constant in [0, π/2]). When there is a maximum in $\theta_1 = \pi/2$, the interaction surface (2) in that particular space will be represented by the equation,

$$T + 2QR_0 - W\sigma_e/\sqrt{3} = 0. \quad (9)$$

$$\text{(b)} \quad f''(\theta_2) = \left[\left(24Q^2R_0^2 - 8F^2\right)\cos 2\theta_2 - 12TQR_0\sin\theta_2\right]/W^2 < 0,$$

where, on replacing Eq. (5) and after performing some operations, this gives

$$\left(F^2 - 3Q^2R_0^2\right)\left[4\left(F^2 - 3Q^2R_0^2\right)^2 - 9T^2Q^2R_0^2\right] > 0. \tag{10}$$

Only in the space region (T, F, Q) satisfying Eq. (10) are we going to have a maximum in θ_2. In that case, the interaction surface is represented by the equation obtained by replacing Eq. (5) with Eq. (2), which after some operations, becomes

$$4F^6 - 24F^4Q^2R_0^2 + 36F^2Q^4R_0^4 - 9T^2Q^2R_0^2F^2 + 3T^2F^4 - 9\sigma_e^2W^2Q^4R_0^4 + 6\sigma_e^2W^2F^2Q^2R_0^2 - \sigma_e^2W^2F^4 = 0. \tag{11}$$

3. Geometric interpretation and discussion of the problem

3.1. Regions corresponding to each maximum situation

The (T, F, Q) space regions in which the position of the maximum of $f(\theta)$ becomes explicit by Eq. (4) or Eq. (5) are delimited by inequalities (8) and (10), respectively.

Next, the characteristics of these regions will be described. However, a detailed analysis will not be given as it is beyond the reasonable scope of this paper.

3.1.1. Maximum in $\theta_1 = \pi/2$

Inequality (8) is satisfied by the (T, F, Q) points, internal in that space to a C_1 cone with an elliptical guideline, a vertex in the origin and an axis contained in the TQ plane. One of whose generatrices is the OT axis, represented in Fig. 2.

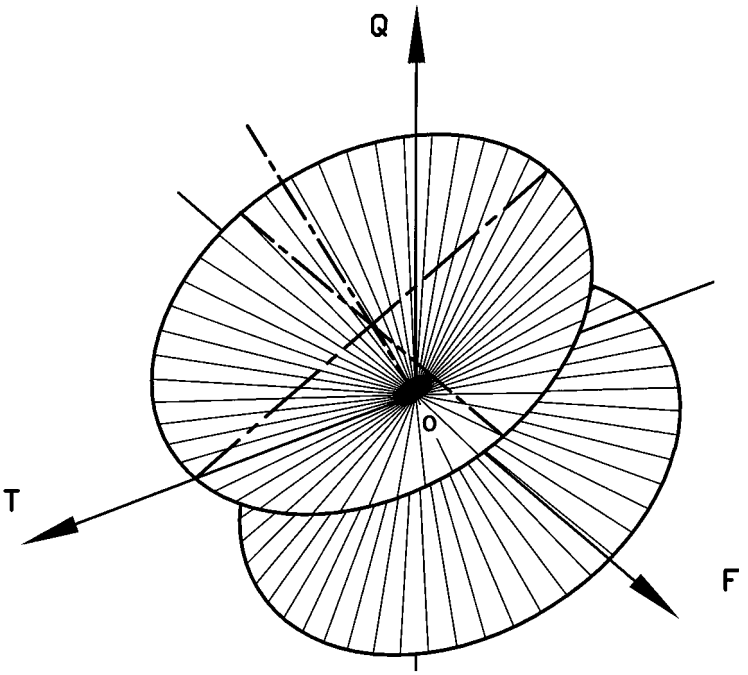

Fig. 2. The C_1 cone.

For points located inside that cone, the maximum value of $f(\theta)$ is reached in $\theta_1 = \pi/2$, whereas, outside the cone, a minimum value of f appears at the same point.

3.1.2. Maximum in $\theta_2 = arcsin\left[3TQR_0/\left(2F^2 - 6Q^2R_0^2\right)\right]$

It can be demonstrated that inequality (10) is satisfied:

(a) In the (T, F, Q) points being outside the C_1 cone, and on the half space $F > \sqrt{3}QR_0$ (Fig. 3) simultaneously.

(b) In the points (T, F, Q) being (i) outside the C_2 cone, symmetric to the C_1 cone with respect to the FQ plane; (ii) on the half space $F < \sqrt{3}QR_0$ (Fig. 3) simultaneously.

If the study is restricted to the first octant in the T, F, Q space (without making the problem less general, given its symmetries), all these conditions are summarized in a single condition: the (T, F, Q) combination is outside the C_1 cone. This occurs because, in the above mentioned octant, the second condition of (a) is included in the first one, and the region inside it that fulfills (b), remains inside the C_1 cone, where according to Eq. (6b), the solution θ_2 of Eq. (3) is not real.

In a summary, at (T, F, Q) points inside the C_1 cone, the maximum of $f(\theta)$ is reached at θ_1, and outside the cone, the maximum of $f(\theta)$ is reached at θ_2. Whereas precisely on its surface, from Eqs. (4) and (5), it occurs that $\theta_2 = \theta_1$, and there is a continuous variation of the position for the maximum.

3.2. Study of the limit surface for the maximum in θ_1

When the maximum of $f(\theta)$ is reached in θ_1, the limit interaction surface is given by Eq. (9).

This surface is a plane in the (T, F, Q) space, parallel to the cone back generatrix, which cuts the C_1 cone into a parabola as it is shown in Fig. 4. Its field of validity is limited to the inner part of the cone, in other words, to the portion represented in the figure. The surface is independent of F because the bending stress is zero at θ_1. The parabola is given by the system of Eq. (9) and $C_1 = 0$ in Eq. (8).

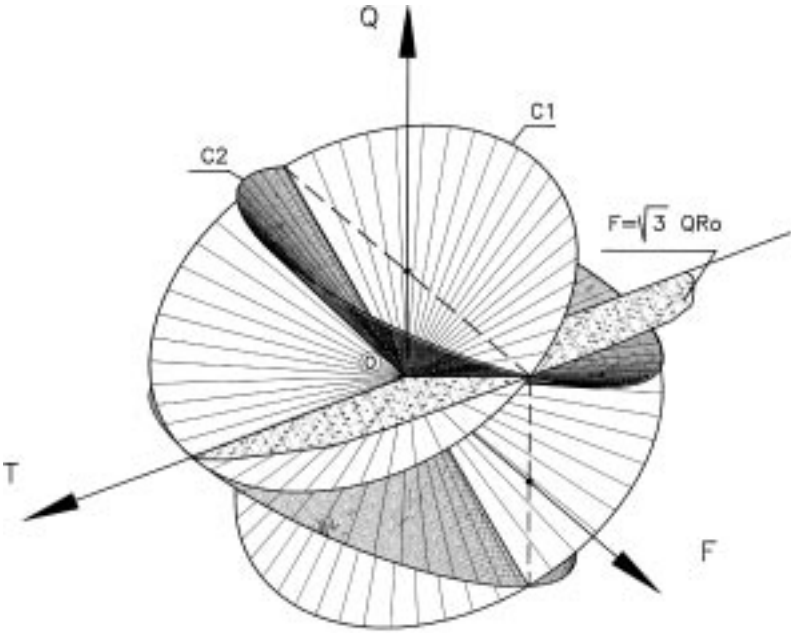

Fig. 3. Intersection of C_1 and C_2 cones with plane $F = \sqrt{3}R_0Q$.

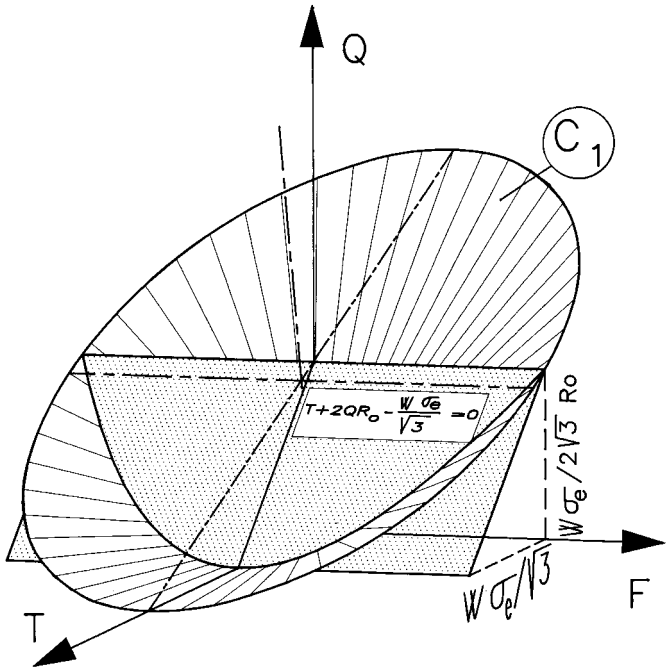

Fig. 4. The limit surface for maximum in θ_1.

3.3. Study of the limit surface for the maximum in θ_2

When the maximum of $f(\theta)$ is reached at θ_2, the limit interaction surface is given by Eq. (11).

This surface, considerably more complex than the previous one, becomes the interaction surface outside the C_1 cone.

Although a detailed account cannot be given in this study, some conclusions could be offered, which are the following:

Expression (11) can be factorised as

$$\left(F^2 - 3R_0^2Q^2\right)\left[4F^4 + F^2\left(3T^2 - 12R_0^2Q^2 - W^2\sigma_e^2\right) + 3W^2\sigma_e^2R_0^2Q^2\right] = 0. \tag{12}$$

Surface (11) consists of three sheets, two of them flat. The third sheet shows, in general, a double curvature and, in turn, is divided into six regions: four of them are open and not fenced in, whereas two of them are closed and fenced in, symmetric in pairs with respect to the TQ plane. In fact, the surface is symmetric with respect to the three coordinate planes and meets the origin and several straight lines in its course.

Of surface (11), only the portion of the closed regions contained in the first octant, affects the problem's range. In Fig. 5, the portion's contour line seen from the three projections and a perspective are represented, which gives an idea of its shape.

The plane given by Eq. (9), which constitutes the interaction surface in the case of maximum in $\theta_1 = \pi/2$, is tangent to surface (11) along a parabola coinciding with the intersection of that plane with the C_1 cone.

The surface closed regions are contained in a cylinder with a vertical Q axis, whose guideline is the ellipse forming the intersection of the surface with the $Q = 0$ plane, and along which the surface and the cylinder are tangent.

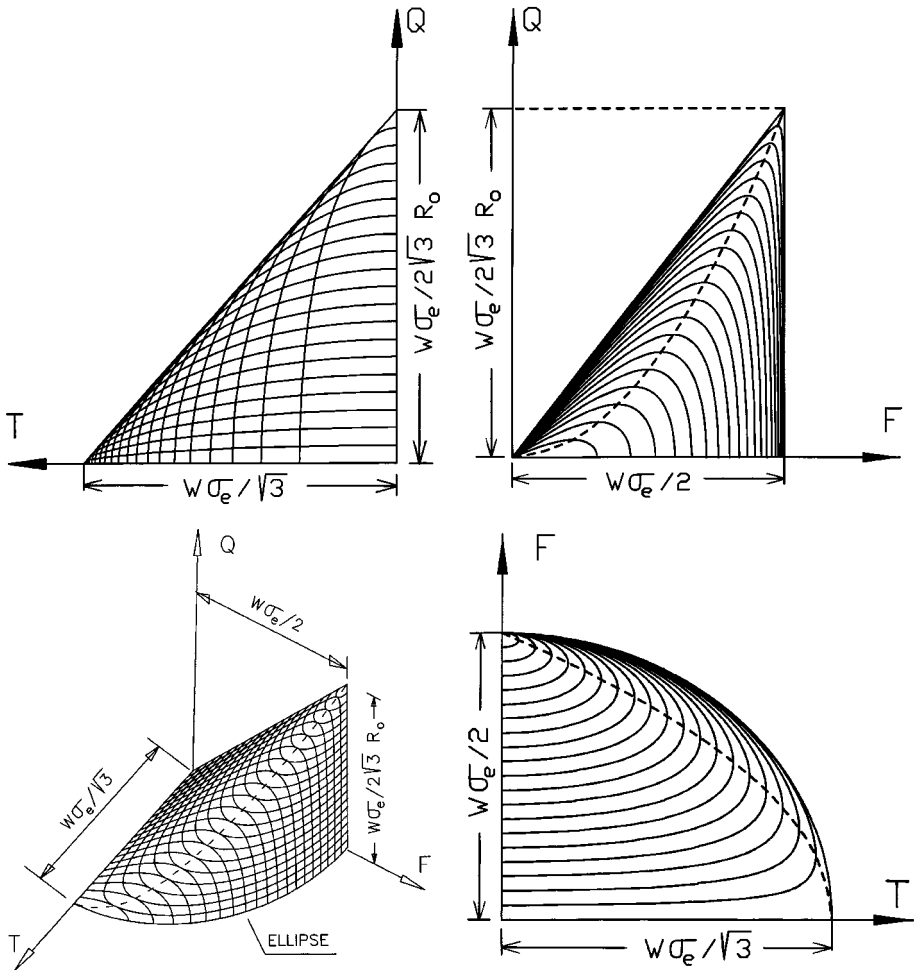

Fig. 5. The closed region of surface (11) affecting the problem.

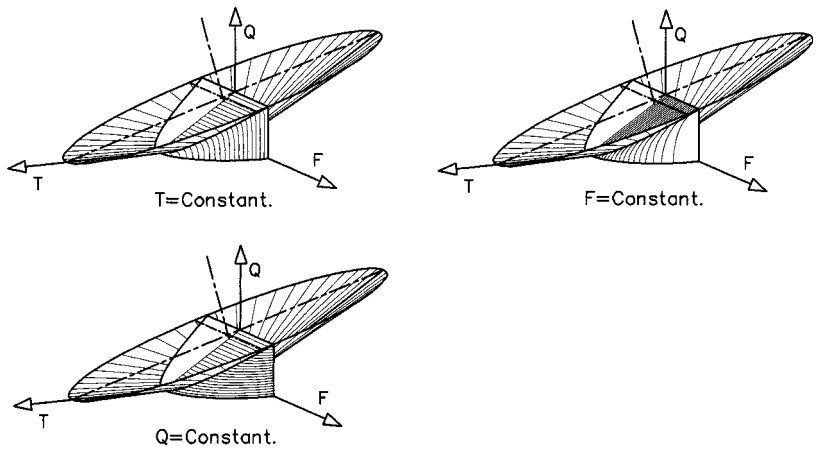

Fig. 6. Generation of possible interaction diagrams.

Therefore, the validity region of the surface for the problem corresponds to its portion in the first octant, external to the C_1 cone, for which that surface also cuts according to the same parabola.

It can also be seen (see García and López (1984) or any other Algebra treatise) that in a (T^2, F^2, Q^2) space the plane part of the limit surface in the (T, F, Q) space becomes a cylinder with conical directrix, and the curved part becomes an hyperbolic paraboloid but this representation seems less interesting from the point of view of obtaining interaction diagrams.

4. Representation of the limit surface: interaction diagrams

The limit surface is constituted by two regions, one of them flat and the other curved, but with a continuity of value and of first derivatives in all directions throughout the common parabola. Taking this

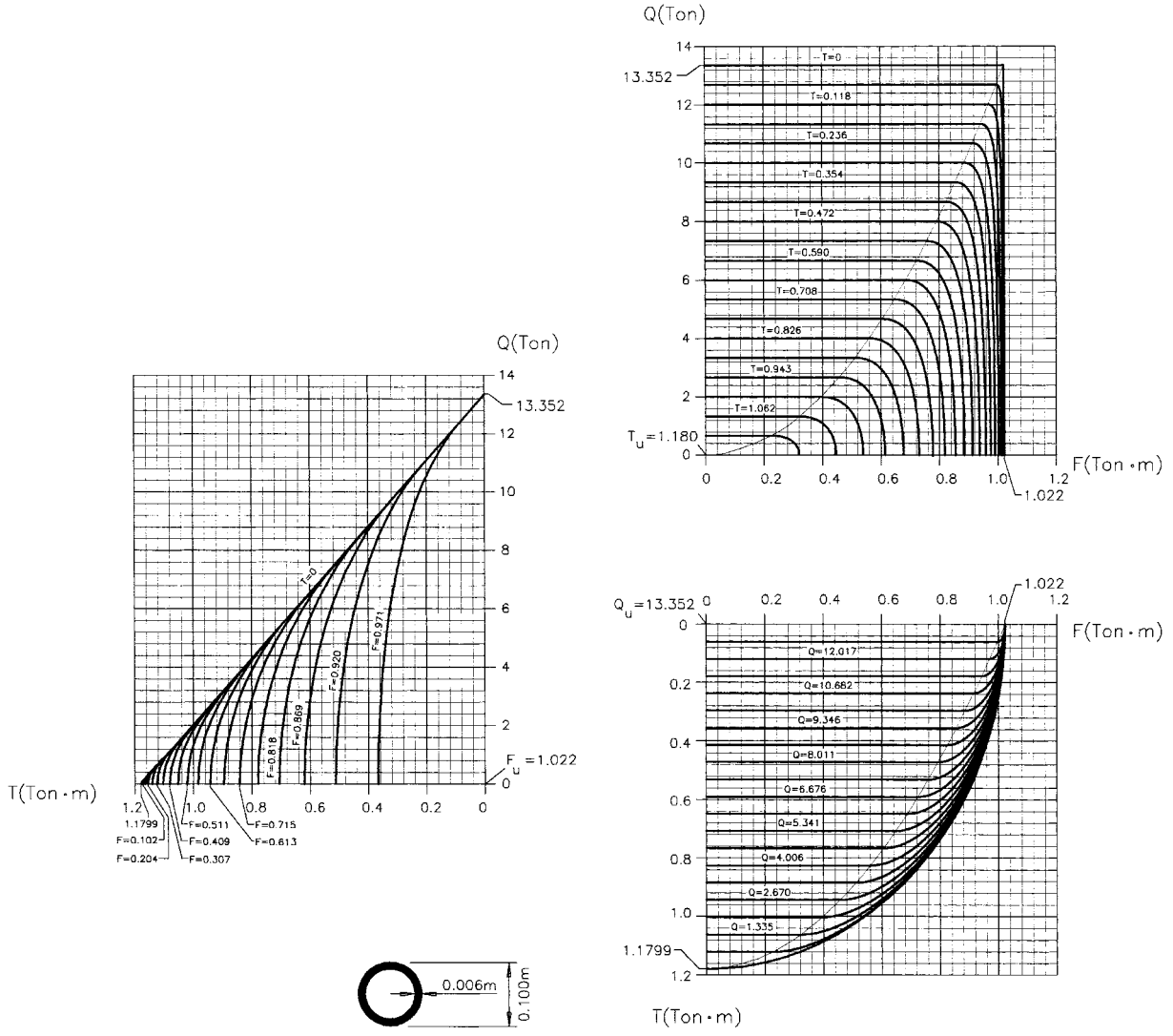

Fig. 7. Interaction graphs for a profile with $R = 50$ mm and $t = 6$ mm ($\sigma_e = 254.8 \times 10^6$ Pa).

into account, all the possible interaction diagrams representing their contour lines according to planes parallel to the coordinate ones will be made up of mixed lines with a straight part and a curved one. The latter would have a different nature depending on the section being considered, as well as the continuity of value of the first derivative in the confluence point.

Fig. 6 shows the generation of the three possible diagrams for the different sections indicated. The lines corresponding to sections where $F =$ constant, are made of straight and elliptic parts. In the other two cases ($T =$ constant or $Q =$ constant), the curved stretch is represented by more complex fourth degree equations. However, one of the variables can be made explicit.

In Fig. 7, three possible interaction diagrams are represented for a supposed section with $R = 50$ mm and $t = 6$ mm of a steel with $\sigma_e = 254.8 \times 10^6$ Pa, ready to be used.

5. Conclusion

This paper deals with the analytical formulation for obtaining the yield limit interaction surface for the shear, bending and torsional stresses in circular hollow metallic sections.

The surface consists of a flat part and a warped one, in the corresponding shear–bending–torsion space.

A complete discussion of the problem is offered in which exclusively analytical techniques have been used. These techniques are more or less complex depending on the characteristics of each region in the surface.

The examination of the surface shows that except for torsion and bending (T, F) pairs near their maximum values, the surface is independent of the bending action.

As an example, interaction diagrams have been provided for a section with $R = 50$ mm and $t = 6$ mm.

References

García, J., López, M., 1984. Algebra Lineal y Geometría. th Ed. Marfil. Alcoy, Spain.

Irles, R., Irles, F., 2000. Elastic Interaction Graphs for Steel H-sections subjected to Bending, Shear and Axial Forces. Int. J. Solids Struct. 37, 1327–1337.